Journal of Innovative Optical Health Sciences
Vol. 2, No. 4 (2009) 407–422

World Scientific
www.worldscientific.com

IN VIVO NEAR-INFRARED FLUORESCENCE IMAGING OF HUMAN COLON ADENOCARCINOMA BY SPECIFIC IMMUNOTARGETING OF A TUMOR-ASSOCIATED MUCIN

RALPH S. DACOSTA[*,††], YING TANG[‡],
TUULA KALLIOMAKI[†], RAYMOND M. REILLY[§], ROBERT WEERSINK[¶],
ALISHA R. ELFORD[‖], NORMAN E. MARCON[**] and BRIAN C. WILSON[†]

[*]*Division of Biophysics and Bioimaging, Ontario Cancer Institute*
610 University of Toronto, Toronto, Ontario, M5G 2M9, Canada

[†]*Department of Medical Biophysics, University of Toronto*
Princess Margaret Hospital/Ontario Cancer Institute
University Health Network, Toronto, Ontario, Canada

[‡]*NIH/NCI, Radiation Oncology Branch*
Bethesda, MD, USA

[§]*Division of Clinical Investigation and Human Physiology*
Toronto General Hospital Research Institute, and University of Toronto
Leslie Dan Faculty of Pharmacy Toronto, Ontario, Canada

[¶]*Laboratory for Applied Biophotonics*
University Health Network, Toronto, Ontario, Canada

[‖]*Campbell Family Institute for Breast Cancer Research*
University Health Network/Ontario Cancer Institute
Department of Medical Biophysics and Immunology
Toronto, Ontario, Canada

[**]*St. Michael's Hospital*
Center for Therapeutic Endoscopy and Endoscopic Oncology
Toronto, Ontario, Canada
[††]*rdacosta@uhnres.utoronto.ca*

Background and Aims: Accurate endoscopic detection of premalignant lesions and early cancers in the colon is essential for cure, since prognosis is closely related to lesion size and stage. Although it has great clinical potential, autofluorescence endoscopy has limited tumor-to-normal tissue image contrast for detecting small preneoplastic lesions. We have developed a molecularly specific, near-infrared fluorescent monoclonal antibody (CC49) bioconjugate which targets tumor-associated glycoprotein 72 (TAG72), as a contrast agent to improve fluorescence-based endoscopy of colon cancer. **Methods:** The fluorescent anti-TAG72 conjugate was evaluated *in vitro* and *in vivo* in athymic nude mice bearing human colon adenocarcinoma (LS174T) subcutaneous tumors. Autofluorescence, a fluorescent but irrelevant antibody and the free fluorescent dye served as controls. Fluorescent agents were injected intravenously, and *in vivo* whole body fluorescence imaging was performed at various time points to determine pharmacokinetics, followed by *ex vivo* tissue analysis by confocal fluorescence microscopy and histology.

[††]Corresponding author.

Results: Fluorescence microscopy and histology confirmed specific LS174T cell membrane targeting of labeled CC49 *in vitro* and *ex vivo*. *In vivo* fluorescence imaging demonstrated significant tumor-to-normal tissue contrast enhancement with labeled-CC49 at three hours post injection, with maximum contrast after 48 h. Accumulation of tumor fluorescence demonstrated that modification of CC49 antibodies did not alter their specific tumor-localizing properties, and was antibody-dependent since controls did not produce detectable tumor fluorescence. **Conclusions:** These results show proof-of-principle that our near-infrared fluorescent-antibody probe targeting a tumor-associated mucin detects colonic tumors at the molecular level in real time, and offer a basis for future improvement of image contrast during clinical fluorescence endoscopy.

Keywords: Autofluorescence imaging; endoscopy; colon adenocarcinoma; TAG72; CC49; mucin; monoclonal antibody; conjugate; confocal fluorescence microscopy.

1. Introduction

Endoscopic detection of early preneoplastic lesions is critical to improving the cure rate of colon cancer.[1] Conventional white-light endoscopy (WLE) in the colon detects large benign hyperplastic polyps and preneoplastic adenomatous polyps (>5 mm diameter) before they reach advanced cancer stage.[2] However, it is difficult to detect smaller and early preneoplastic lesions, detect flat adenomas, or identify lesion boundaries with WLE.

In our ongoing clinical studies, light-induced fluorescence endoscopic (LIFE) imaging was used *in vivo*, adjunctively with WLE, to detect hyperplastic and adenomatous polyps, based on tissue autofluorescence.[3] With LIFE imaging using blue-light excitation, adenomatous polyps have red-shifted fluorescence compared with normal colon or benign hyperplastic lesions, resulting in a contrast image.[4] These differences are due primarily to local concentration changes in intrinsic fluorescent biomolecules [i.e., collagen, elastin and the metabolic coenzymes nicotinamide adenine dinucleotide (NADH) and flavins], to altered microvascularity and to changes in mucosal layer thickness associated with neoplastic transformation, the latter two factors altering the tissue light attenuation. However, despite significant technological advantages as well as growing clinical expertise using autofluorescence endoscopy,[3,5,6] there is still room for improvement in the fluorescence contrast between preneoplastic lesions and surrounding background normal tissue. Hence, there is continued interest in developing contrast agents to increase the detection sensitivity and specificity of colonic adenomas.

Clinical studies have been reported[7–9] using sub-therapeutic doses of the exogenous prodrug aminolevulinic acid (ALA) which leads to selective synthesis of fluorescent protoporphyrin IX (PpIX) in some tumors and is commonly used in photodynamic therapy.[10–12] However, in the colon this had an unacceptable false-positive rate, associated with microscopic inflammation of the mucosa or feces in the colon.[13] Here we have investigated, in a pre-clinical model, the strategy of using an exogenous fluorescent agent that is specifically targeted to a known tumor-associated antigen.

Changes in mucin glycoproteins are one of the most common phenotypic markers of colorectal carcinogenesis, play an important pathobiological role and may offer a means to specifically target colonic neoplastic lesions. In colonic epithelial cancers, both qualitative and quantitative alterations occur in carbohydrate and polypeptide moieties of mucin glycoproteins. The expression of some of these antigens appears to correlate with poor prognosis and increased metastatic potential.[14,15] The increased exposure of mucin glycoproteins in colorectal cancer cells appears to be associated with aberrant glycosylation, altered levels of mucin gene transcription and/or dysregulation of tissue specific mucin genes.[15–20] Monoclonal antibodies (MAbs) have been developed against some of the carbohydrate epitopes. CC49 is one such MAb that recognizes the tumor-associated glycoprotein-72 (TAG72). TAG72 is a high–molecular-weight glycoprotein (220–400 kDa) that localizes to the cytoplasm and cell membrane of malignant cells. Most human adenocarcinomas, including breast, colon, gastric, ovarian, prostate and lung, express TAG72, recognizable by the CC49 antibody,[21] but these mucins are rarely expressed in normal epithelium or benign tissues.[22] In addition, the widespread distribution of the antigen on malignant cells makes the CC49 MAb a potentially powerful

tool for various immunodiagnostic and therapeutic purposes.[23] In particular, for our purposes, CC49 MAbs directed against TAG72 offer an opportunity to selectively deliver a fluorescent dye to tumor cells for targeted "immunophotodetection" of preneoplastic and neoplastic lesions.

Over the past 20 years, "proof-of-principle" has been clearly shown for specific radioimmunodetection (RID) of tumors using radiolabeled MAbs directed against tumor-associated epitopes.[24,25] Moreover, such nuclear medicine imaging has been used in conjunction with radiolabeled MAbs intended for treatment of tumors (radioimmunotherapy) and for prediction of radiation absorbed doses to tumors and normal tissues.[26–30] RID has advantages in terms of sensitivity for probing tumor-associated epitope expression in lesions throughout the body but is limited by its relatively poor spatial resolution (0.5–1 cm). Fluorescence-based imaging offers a form of imaging that is more convenient, less expensive and of much higher resolution, which can be applied to localized anatomic regions (e.g., endoscopy).

Adapting the immunotargeting principle for fluorescence imaging involves the conjugation of a fluorophore dye to a MAb or other tumor-targeting moiety. Typically, fluorophores used for this purpose are excited in the red spectral range (∼600–700 nm) with near-infrared (NIR) fluorescence emission. The main advantage of using these longer wavelengths is reduced background tissue autofluorescence. Dyes are available with adequate stability for *in vivo* imaging and produce fluorescence that is detectable through millimeter thicknesses of tissues.[31,32] Recent improvements in MAbs or MAb fragments,[33] the commercial availability of NIR-emitting fluorophores and the availability of high-sensitivity digital cameras in this spectral region have made tumor-localization using NIR-fluorescence contrast agents practical and attractive.

In this report, we describe the use of a commercially-available, NIR fluorescent dye, AlexaFluor647^{TM} (Molecular Probes, Oregon, USA), which we conjugated to the CC49 MAb with a high affinity ($K_a = 1.6 \times 10^{10}$ M^{-1}) for the TAG72 antigen expressed in up to ∼94% of human colorectal tumors,[34] and evaluated this construct *in vitro* in human colon tumor cells and then *in vivo* and *ex vivo* with the cells grown as solid tumors in a xenograft nude mouse model.

2. Materials and Methods

2.1. *Establishment of colon cancer xenografts*

LS174T human colon cancer cells were obtained from the American Type Culture Collection (Rockville, MD, USA) and were grown in Eagle's Minimal Essential Medium supplemented with 10% fetal calf serum (Sigma, St. Louis, MO, USA) at 37°C in a humidified environment containing 5% CO_2. Sub-confluent cells were harvested by trypsinization with 0.25% trypsin/EDTA (Sigma, St. Louis, MO, USA). Cells were centrifuged at 300× g for ∼5 minutes and then re-suspended in sterile NaCl (150 mmol/L). Approximately 2×10^6 cells were injected subcutaneously in the right hind leg (flank) of 6–8 week-old female (∼20 g) Swiss athymic (nu/nu) mice ($n = 11$) (Taconic, Germantown, NY). Animals were maintained in the Animal Resource Centre of the Ontario Cancer Institute/Princess Margaret Hospital in compliance with the guidelines of the Canadian Counsel on Animal Care, and animal procedures were performed according to an animal use protocol (AUP) approved by University Health Network, Toronto (No. TG:00-026). Tumors were allowed to reach a diameter of ∼5–12 mm before the *in vivo* imaging studies (∼12–14 days). During this time, mice were fed autoclaved rodent diet (Cat. #5010, LabDiet, St. Louis, Missouri, USA) and sterilized water.

2.2. *Relevant monoclonal antibody*

The anti-TAG72 murine CC49 MAb was selected as the relevant test monoclonal antibody. Mouse ascites containing the second-generation TAG72 MAb CC49 (IgG1) were generously provided by Dr. J. Schlom, National Institutes of Health (Bethesda, MD, USA). CC49 MAb was purified from the ascites on a Protein G agarose affinity column (Pierce, Rockford, IL, USA), then desalted on a PD-10 Sephadex G-25 column (Pharmacia, Baie d'Urfe, PQ, Canada), and eluted with 50 mmol/L sodium bicarbonate in 150 mmol/L NaCl at pH 7.5. Pure CC49 MAb was concentrated to 10 mg/mL on a Centricon-30 ultra-filtration device (Amicon, Beverly, MA, USA). The purity of the CC49 MAb was confirmed by sodium dodecylsulphate polyacrylamide gel electrophoresis (SDS-PAGE) on a 4–20% Tris-glycine gradient gel (BioRad, Hercules, CA, USA) stained with Coomassie R-250 blue

(BioRad), which showed a single band corresponding to a protein with the expected M_r of 150 kDa.

2.3. *Irrelevant monoclonal antibody*

Humanized M195 (HuM195) MAb was selected as the irrelevant monoclonal antibody for these experiments. This is a genetically engineered, human IgG_1 version of the parent M195, a mouse IgG_{2a} anti-CD33 MAb. CD33 is a 67-kD cell-surface glycoprotein found on most myeloid leukemia cells and on committed myelomonocytic and erythroid progenitor cells. HuM195 MAb was obtained from PDL (Protein Design Labs, Fremont, CA).

2.4. *Preparation and characterization of fluorescent contrast agents*

Conjugation of monoclonal antibodies was performed using an AlexaFluor647^{TM} MAb labeling kit (A-20186, Molecular Probes, Eugene, OR, USA) according to the manufacturer's instructions. AlexaFluor647^{TM} has a maximum absorption at 650 nm and a maximum fluorescence emission at 668 nm. AlexaFluor647^{TM} reactivity with proteins is based on the reactivity of the succinimidyl esters with reactive primary amine groups of the MAb. Briefly, approximately 100 μg each of CC49 and M195 MAbs in appropriate buffers, free of ammonium ions or primary amines, was used for conjugation. Each antibody solution was buffered by 1 M sodium bicarbonate buffer (Molecular Probes) at a concentration of 1 mg/mL and $\sim$100 μL was added to a vial containing the amine-reactive AlexaFluor647^{TM} dye. The vials were capped and gently inverted several times to fully dissolve the dye, but avoiding excessive agitation. They were then incubated for one hour at room temperature during which they were gently inverted every 10–15 minutes to mix the reactants. Unbound dye was removed by using size-exclusion spin columns optimized for proteins >30 kDa (Molecular Probes). The 100 μL reaction volume was added dropwise onto the center of the spin column and allowed to absorb into the gel bed. The column was then centrifuged for five minutes at 1,100 $\times$ g. Thereby, either labeled CC49 or labeled M195 MAbs was obtained in approximately 100 μL of phosphate buffered saline (PBS) adjusted to pH 7.2, with 2 mM sodium azide.

In order to determine the concentration of protein in the sample and the labeling ratio (moles of fluorescent dye/MAb), a small measured amount of the purified conjugate (either CC49 or M195) was diluted in a known volume of PBS in a 1-cm pathlength quartz cuvette and the optical absorbance was measured at both 280 nm (mainly IgG) and 650 nm (AlexaFluor647^{TM}). The protein concentration (Molarity) was then calculated by the following:

$$P(M) = \frac{[A_{280} - (A_{650} \times 0.03)] \cdot (\textit{dilution factor})}{203{,}000}, \tag{1}$$

where the *factor* 203,000 is the molar extinction coefficient in $cm^{-1}M^{-1}$ of IgG at 280 nm and 0.03 is a correction factor for the fluorophore absorption at 280 nm. For labeled CC49 and M195, each vial contained 97 μg/100 μL and 95 μg/100 μL of protein, respectively. Equation (2) was then used to calculate the degree of conjugate labeling:

$$\text{Moles of dye per mole of protein} = \frac{A_{650} \times \textit{dilution factor}}{239{,}000 \times \text{protein concentration (M)}}, \tag{2}$$

where 239,000 $cm^{-1}M^{-1}$ is the molar extinction coefficient of AlexaFluor647^{TM} at 650 nm. Conjugated CC49 and M195 were labeled at $\sim$5.8 and 4.8 moles of AlexaFluor647^{TM} to 1 mole of CC49, respectively, which are within the optimal range (4–9) for IgG labeling specified by the kit manufacturer. The labeled MAbs were protected from light by wrapping the vials in aluminum foil, and stored at 4°C until used. Their optical absorption and fluorescence emission spectra were confirmed to be the same as those of free AlexaFluor647^{TM}, as determined using a UV-VIS spectrophotometer (Model UV-160U, Shimadzu, Pleasanton, CA, USA), and a scanning spectrofluorimeter (Model PTI LS-101, Photon Technologies Inc., Lawrenceville, NJ, USA), respectively.

2.5. *In vitro binding studies of AlexaFluor647^{TM} bioconjugates*

The specificities of the relevant (CC49) and irrelevant (M195) conjugates for the LS174T cell line were examined using confocal fluorescence microscopy (CFM) *in vitro*. Under sterile conditions, LS174T cells ($\sim$20 μL of a 1 $\times$ 10^4 cells/mL suspension) were seeded in 8-well chambered coverslip plates (Nunc, Sigma Aldrich, Oakville, ON,

Canada) and incubated in Eagle's Minimal Essential Medium supplemented with 10% fetal calf serum and antibiotics (Sigma) (at $\sim$300 μL/well) overnight, at 37°C in a humidified environment containing 5% CO_2. Conjugated CC49 (final concentration 0.02 μg/μL), conjugated M195 (0.02 μg/μL) or free AlexaFluor647^{TM} dye (unconjugated) was added to the culture medium in each well and the cells were incubated with the agents for a further 30 minutes. Prior to CFM imaging, the culture media containing the unbound agents were removed from the wells and cells were gently washed three times with ice-cold PBS. CFM was performed on a Zeiss LSM 510 instrument (Carl Zeiss, Jena, Germany) on both single cells and cell colonies, using 635 nm excitation from a HeNe laser and detecting the AlexaFluor647^{TM} fluorescence emission at 650–710 nm (*false-colored red*). Confocal fluorescence micrographs (8-bit, 1024 × 1024 pixels, average of 4 scans/image) were collected, with the pinhole size, laser intensity and detector gain settings optimized and kept constant for all imaging procedures. Transmitted light images were also collected for comparison of cell morphology. In addition, reconstructed 3D CFM images were used to determine qualitatively the binding specificity and distribution of the conjugated CC49 probe on the cell surface. For this, serial confocal sections were collected and 3D projections were rendered using the Zeiss Image Analysis software package. As a further control, two wells received no agents and the background cellular autofluorescence was imaged.

2.6. *In vivo NIR fluorescence imaging*

Autofluorescence images were acquired from two tumor-bearing controls which were not injected with any agent. Three groups of three mice each were given equal intravenous (*iv*) doses ($\sim$30 μg conjugate/animal) of AlexFluor647^{TM}-conjugated CC49, AlexFluor647^{TM}-conjugated M195 or unconjugated free dye, via the tail vein. The mice were anesthetized by subcutaneous injection (0.1 mL of stock anesthetic solution containing 6.7 mL saline, 2.5 mL ketamine, 0.6 mL xylazine and 0.25 mL acepromazine) and a butterfly catheter was placed in the tail vein for *iv* bolus injections of the fluorescent probes. The mice were then imaged, using a stereo epifluorescence microscope (MZ FLIII, Leica Microsystems, Richmond Hill, ON, Canada) equipped with a 16-bit, C-mounted ICCD camera (Model DH510, Andor Technology, South Winsdor, CT, USA) at 0, 3, 24, 48, and 72 hours later. Excitation at 635 ± 2 nm from a home-built diode laser source (Laboratory for Applied Biophotonics, Toronto, ON, Canada) illuminated the dorsal or abdominal surface using an optical fiber bundle with a diverging lens to expand the beam to a 9-cm diameter circle at a power density of 20 mW/cm^2. The illumination field was homogenous to ±10% over a 10 × 10 cm area, and adequately illuminated the tumor and surrounding normal tissues. White-light images were acquired by illuminating the dorsal surface using a 50-W mercury arc lamp (Leica) for anatomical comparison. Whole body fluorescence imaging was performed in a darkened room using a longpass (>670 nm) filter (Chroma Technology Corp., Brattleboro, VT, USA) fitted to the camera lens that blocked any reflected excitation light. Fluorescence images were also acquired from the dorsal side so that both the tumor-bearing and tumor-free hind legs were within the same field of view (FOV). In addition, fluorescence images were collected from the abdominal side of the uninjected control mice to determine any autofluorescence and contrast agent fluorescence level in the gastrointestinal (GI) tract. All fluorescence images were acquired digitally over about three seconds as 16-bit grey-scale TIFF files and captured on a PC using Andor MCD imaging software (Version 5.1, Media Cybernetics, Silver Spring, MD, USA). Fluorescence images were processed and analyzed using MATLAB (The MathWorks Inc., Natick, MA, USA). Briefly, region of interest (ROI) segmentation of a defined area (6-mm diameter circle/0.28 cm^2) was used to determine the average fluorescence intensity per unit area within the tumor boundary and within the same ROI area in normal tissue from the opposite tumor-free hind leg of the same mouse. For each group of mice, the net average tumor fluorescence intensity in the ROI images was calculated by taking the average autofluorescence intensity on the contralateral normal side for all mice and subtracting this from the tumor fluorescence intensity. The results were plotted *versus* time after injection to show the contrast and kinetics of the fluorescent probes *in vivo*.

2.7. *Ex vivo NIR fluorescence imaging*

All mice were sacrificed at 72 hours and organs (stomach, colon, kidneys, liver, heart, spleen, gall

bladder) and tumors were resected carefully and rinsed with PBS to remove excess blood. For each mouse, the freshly excised organs and tumor were placed on a black, non-fluorescent surface and imaged after excision by fluorescence using the stereo epifluorescence microscope. Portions of each tissue were then cut and fixed for one hour in 10% buffered formalin for histology and immunohistological staining. To determine the tissue microdistribution of the fluorescent bioconjugates, samples of normal colon (cleansed of fecal matter by flushing with PBS), muscle and tumor from each mouse were placed quickly in Optimal Cutting Temperature (OCT) compound (Fisher Scientific, Nepean, ON, Canada) and snap-frozen at −80°C. Unstained thin sections (∼5 μm) were cut and mounted on glass microscope slides (Fisher). Drops of inert, non-fluorescent mineral oil (Fisher) were placed on the tissue sections to prevent dehydration and cover slips were applied. This process took about 10 to 15 minutes. The slides were examined immediately using CFM. After fluorescence microscopy, the cover slips and mineral oil were carefully removed and the sections were fixed in 10% buffered formalin for 10 minutes and stained with hematoxylin and eosin (H&E) to correlate the fluorescence microdistribution with the tissue microarchitecture.

2.8. *Histopathology and immunohistochemistry*

Fixed portions (one hour in 10% buffered formalin) of resected tumor and select organs from all mice were embedded in paraffin. Serial 4-μm tissue sections were cut and one section from each sample was stained with H&E. Immunohistochemical staining of tumor, muscle and normal colon samples from tumor-bearing control mice (un-injected with fluorescent agents) was done to compare the intrinsic tumor antigen-expression patterns with the *in vivo* tumor-labeling specificity and microdistribution of the fluorescence conjugates as determined by the CFM imaging of *ex vivo* tissue sections. Staining of paraffinized tissue sections from un-injected control mice was performed according to a standard protocol with a mouse monoclonal anti-TAG72 (SC-20043, Santa Cruz Biotechnology, Santa Cruz, CA, USA) (1:50 dilution overnight) and M195 (1:100 dilution overnight) (Protein Design Labs, Fremont, CA, USA). Negative controls were performed for each MAb by omitting the primary antibody in order to confirm the reactivity. Briefly, for these studies serial 4-μm paraffin sections on microscope slides were de-waxed through five changes of xylene and "brought down" through graded alcohols. Endogenous peroxidase and biotin activities were blocked with hydrogen peroxide solution and an avidin-biotin blocking kit (SP-2001, Vector Laboratories, Burlington, ON, Canada), respectively. Sections were subject to appropriate pre-treatments (for TAG72: pepsin digestion and heat-induced epitope retrieval (HIER) by microwave heating of sections with 10 mM citrate buffer at pH 6.0) inside a pressure cooker (∼20 min) before blocking with protein blocker (ID Labs Biotechnology, London, ON, Canada) for 15 minutes. Sections were then stained for one hour or overnight with the appropriate antibodies at dilutions previously optimized in a moist chamber. Staining was finished by either a catalyzed signal amplification (CSA) system (K1500, Dako Cytomation, Carpinteria, CA, USA) or streptavidin-biotin (IDMR2001, ID Labs) detection systems and developed with either NovaRed (Vector Laboratories, Burlington, Ontario, CAN) or DAB (Dako Cytomation), producing red and brown colors, respectively. Finally, sections were counterstained lightly with Mayer's hematoxylin, dehydrated with graded alcohols, cleared in xylene and mounted in Permount (Fisher).

Imaging of immunohistochemically stained tissue sections was performed under standard white-light microscopy (OPTIPHOT, Nikon, Mississauga, ON, Canada), and images were collected with a color CCD camera (CoolSnap Pro, Houston, TX, USA) using Image Pro Plus Version 5.1 software.

3. Results

3.1. *In vitro targeting*

CFM was used to determine whether AlexaFluor647^{TM} conjugation had any effect on the TAG72 receptor binding characteristics of the CC49 MAb and to demonstrate that the binding specificity of the AlexaFluor647^{TM}-conjugate CC49 is retained after this conjugation. The *in vitro* results are shown in Fig. 1. No significant autofluorescence was observed in the LS174T cells at the wavelengths used (635 nm excitation, 650–710 nm detection), either at the cell surface or intracellularly [Fig. 1(a)]. For comparison, when the following wavelengths were used: 458 nm excitation and 500–550 nm or >560 nm detection, the cells did autofluoresce as expected, showing weak

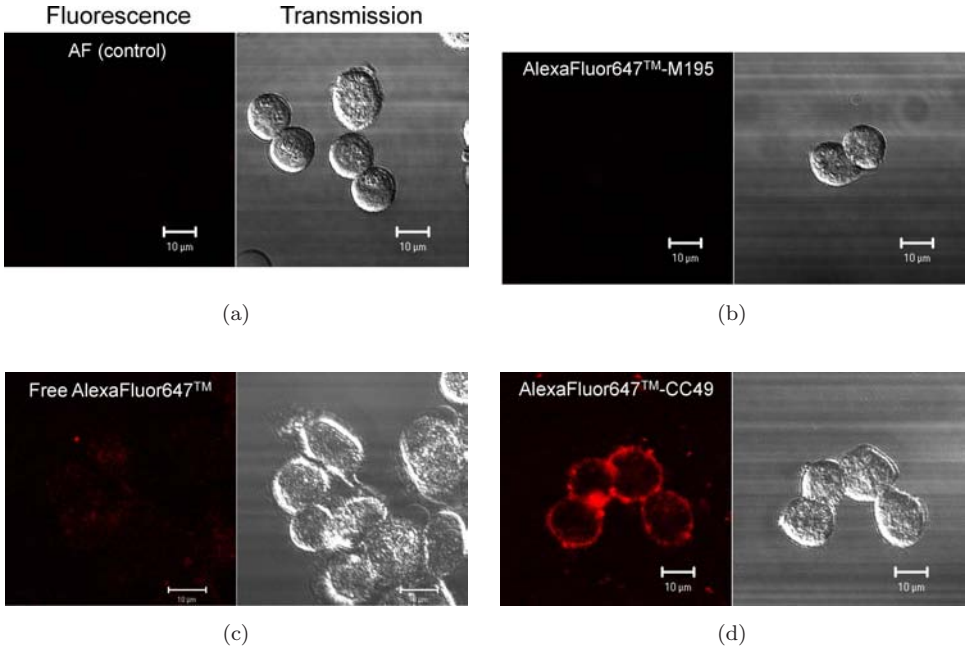

(a) (b) (c) (d)

Fig. 1. Transmission and confocal fluorescence micrographs (635 nm excitation, 650–710 nm emission) of LS174T cells *in vitro* showing (a) autofluorescence, and cells incubated for 0.5 h with (b) AlexaFluor647^{TM}-conjugated M195 (c) free AlexaFluor647^{TM} dye, and (d) AlexaFluor647^{TM}-conjugated CC49.

green fluorescence in the cytoplasm, non-fluorescent nuclei and some bright yellow-orange-red intracellular vesicles, most likely lysosomes.[35] There was no significant red fluorescence in cells incubated with free dye, confirming minimal non-specific labeling [Fig. 1(c)]. By contrast, intense fluorescence was observed at the cell surface of all cells incubated with AlexaFluor647^{TM}+CC49 conjugate, demonstrating specific tumor-antigen targeting [Fig. 1(d)] and no fluorescence for AlexaFluor647^{TM} conjugated with the irrelevant M195 MAb, confirming the specificity of the CC49 conjugate targeting [Fig. 1(b)].

3.2. *In vivo targeting*

Fluorescence imaging was performed with the mice in the dorsal position to image the tumors and in the supine position to image any abdominal fluorescence. In the latter case, all mice (both un-injected and injected) showed strong red fluorescence (635 nm excitation, >670 nm detection) that was most pronounced in the intestines of un-injected control mice, and was attributed to gut contents. Fluorescence images of fresh mouse chow pellets (and their aqueous extract) and excreted feces confirmed this (data not shown), suggesting that future studies should use low-fluorescence mouse chow or mice should be fasted for about 24 hours prior to use. However, since the LS174T tumors studied in these experiments were implanted subcutaneously on the hind leg, the red fluorescence in the intestines caused by the standard mouse chow used here did not affect the results of the tumor contrast imaging.

Figure 2(a) shows a white-light image of the dorsal view of a tumor-bearing mouse, while Fig. 2(b) shows a typical NIR autofluorescence image (635 nm wide-beam excitation, >670 nm emission). The cecum and stomach can be seen in the autofluorescence image while the tumor had low autofluorescence, comparable to the adjacent normal skin. Administration of free AlexaFluor647^{TM} dye did not produce any tumor fluorescence up to 72 hours post injection [Fig. 2(c)] (dye fluorescence was observed in the tail at the injection site in some animals). Similarly, mice injected with the irrelevant AlexaFluor647^{TM}-M195 bioconjugate showed no increase in tumor fluorescence relative to background normal tissue at any of the time points tested up to 72 hours [Fig. 2(d)].

Compared with the control autofluorescence images, the time-course of *in vivo* fluorescence showed distinct contrast enhancement of the tumor against the surrounding normal tissue with the AlexaFluor647^{TM}-CC49 bioconjugate (Fig. 3).

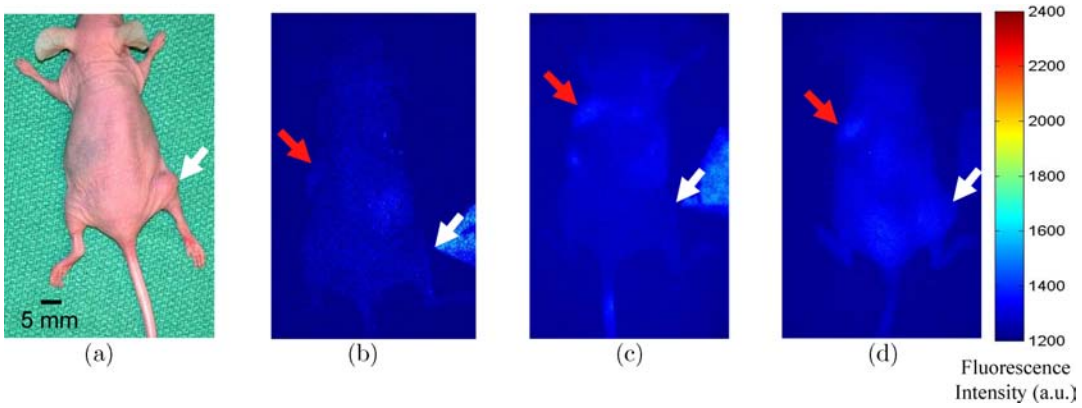

Fig. 2. (a) White-light reflectance image of the dorsal side of an uninjected mouse with LS174T cell tumor (white arrow). (b) Corresponding *in vivo* whole body autofluorescence image (635 nm excitation, >670 nm emission; false colored). Note the absence of any appreciable tumor autofluorescence (white arrows) or tumor fluorescence in mice receiving (c) free AlexaFluor^{TM} dye or (d) AlexaFluor647^{TM}-conjugated M195, but some weak, non-specific fluorescence from internal organs (red arrows).

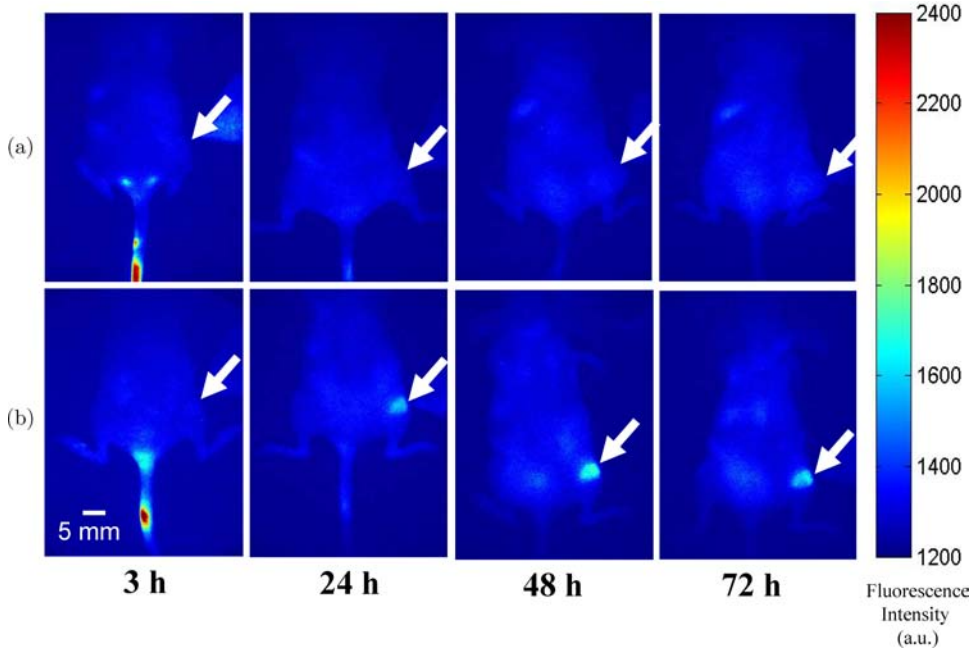

Fig. 3. *In vivo* whole body (635 nm excitation, >670 nm emission; false colored) fluorescence images of the dorsal side at 3, 24, 48 and 72 h after tail vein injection in tumor-bearing (tumor indicated by arrow) mice of (a) AlexaFluor647^{TM}-conjugated M195 MAb, and (b) AlexaFluor647^{TM}-conjugated CC49 MAb.

Immediately after injection, intense fluorescence was observed in the tail, but this cleared after a few hours. Immediately and up to three hours post injection, fluorescence was observed in the vascular-rich preputial glands (Fig. 3), but again this diminished after a few hours, returning to background levels. Tumor fluorescence was apparent as early as three hours and increased to a maximum tumor-to-normal contrast at 48 hours [Fig. 3(b)]. By 72 hours the tumor fluorescence began to decrease. Semiquantitative changes in tumor fluorescence intensities for uninjected and injected mice are depicted in Fig. 4. The highest tumor-to-normal contrast was observed with the CC49 conjugate, peaking at 48 hours.

In one animal with the CC49 conjugate, a small satellite tumor (∼1 mm diameter) was detected adjacent to the primary tumor (Fig. 5). This was also apparent in the white-light image about one week after tumor cell injections. Image segmentation of the grey-scale fluorescence image revealed a high

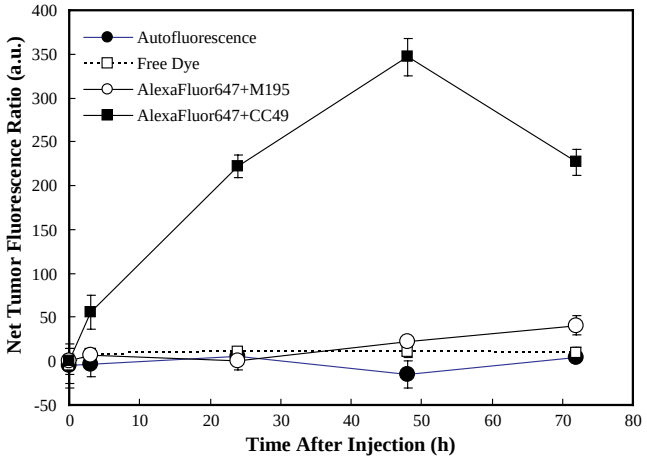

Fig. 4. Tumor contrast (tumor-to-normal tissue ratio: mean ±1 s.d.) as a function of time after *i.v.* administration of the different agents.

signal at the primary tumor site and a distinct but weaker fluorescence intensity at the satellite tumor [Fig. 5(e)].

To determine the tissue distribution of the fluorescence probes, mice were sacrificed at 72 hours and fluorescence imaging was done on the excised organs and tumors using the stereo epifluorescence microscope [Figs. 6(a) and 6(b)]. With 635 nm excitation, intense autofluorescence (668 ± 10 nm) was seen in the stomach, cecum and colon, resulting from porphyrins and chlorophyll in the digested food. This fluorescence was observed in all mice. The tumor fluorescence intensity was highest with the TAG72 targeting probe, compared with no or very weak fluorescence in tumors from un-injected animals or those receiving free dye. However, weak fluorescence was observed only at 72 hours in tumor

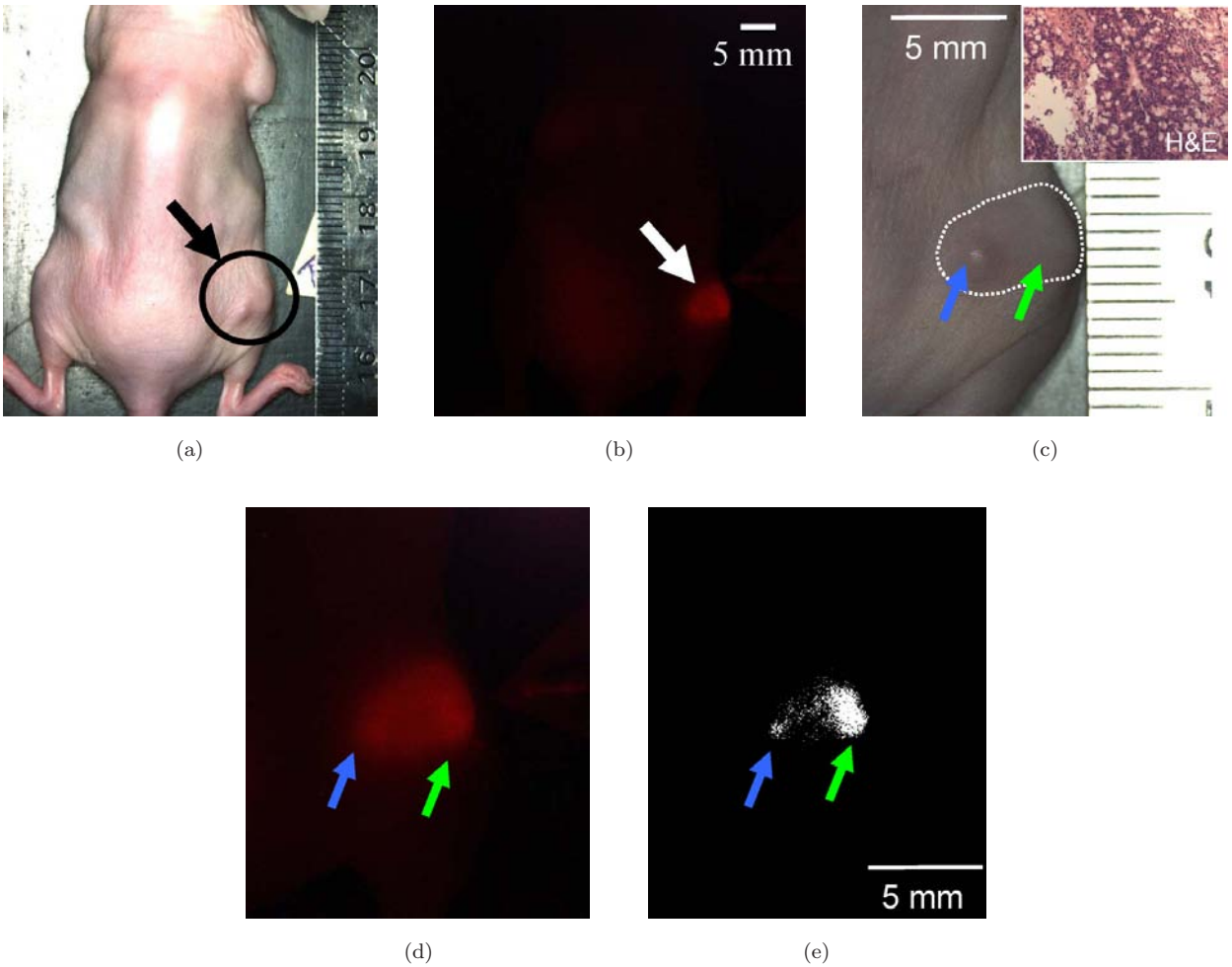

Fig. 5. (a) White-light image of tumor-bearing mouse, and (b) corresponding *in vivo* fluorescence image (635 nm excitation, >670 nm emission) of the same tumor at 72 h post administration of AlexaFluor647^{TM}-CC49 conjugate, (c) one-millimeter diameter satellite tumor (blue arrow) adjacent to the primary xenograft (green arrow), confirmed by H&E-staining (inset), (d) corresponding fluorescence image, and (e) grey-scale intensity-segmented image of the area in (d).

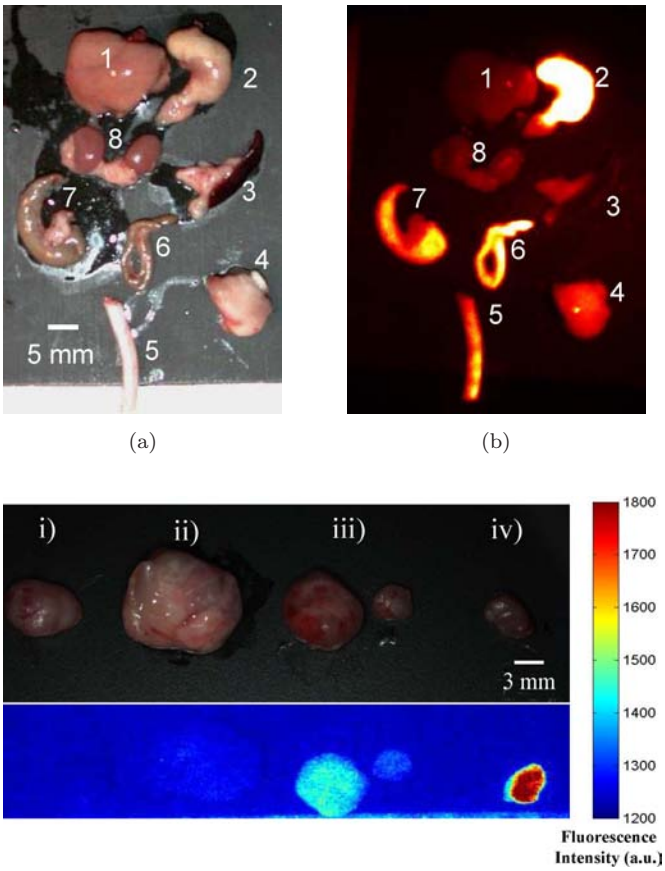

Fig. 6. (a) and (b) White-light and fluorescence (635 nm excitation, 668 ± 10 nm emission) images of excised organs (1-liver, 2-stomach, 3-spleen, 4-tumor, 5-tail, 6-colon, 7-cecum, 8-kidneys) and tumors from a tumor-bearing mouse 72 h after *i.v.* administration of AlexaFluor647^{TM}-CC49 conjugate. (c) White-light image (top) and the corresponding fluorescence micrographs (bottom) of excised LS174T tumors (overlying skin removed) from mice receiving (i) no injection (autofluorescence), (ii) unconjugated free dye, (iii) AlexaFluor647^{TM}-M195 conjugate and (iv) AlexaFluor647^{TM}-CC49 conjugate, all at 72 h.

from one of the three mice with the irrelevant M195 probe, suggesting slight non-specific accumulation. Intravenous bolus administration of ∼30 μg conjugated MAbs (CC49 and M195) as well as free dye to tumor-bearing mice showed no apparent toxicity up to the maximum time point of observation (72 hours).

3.3. *Ex vivo fluorescence confocal microscopy and immunohistochemistry*

High-resolution CFM was performed on unfixed frozen tissue sections from excised normal colon and LS174T tumors from all animals. We chose normal colon to check for cross-reactivity of the AlexaFluor647^{TM}+CC49 conjugates with any endogenous TAG72 receptors found in normal colonic epithelial cells. No appreciable fluorescence from the fluorescent probe was observed in the normal colon [Figs. 7(a) and 7(b)]. However, some fluorescence was observed at the base of the normal mucosa, which we have attributed previously to autofluorescent endogenous endocrine cells.[36] Intense fluorescence was observed throughout the tumor cross sections, and CFM imaging demonstrated specific labeling of tumor epithelial cells with conjugated CC49 [Figs. 7(c) and 7(d)]. Additionally, fluorescence from conjugated-CC49 was observed within tumor neovasculature (Fig. 7). Anti-TAG72 MAb immunohistochemistry with CC49 MAb of *ex vivo* normal colon and LS174T tumors from un-injected control mice showed strong positive staining of tumor cell membranes and mucin vacuoles throughout the tumor, although not all the tumor cells were positively stained [Fig. 7(e)] negligible TAG72 staining was observed in normal colonic epithelia. Light microscopy of a tumor section stained with anti-TAG72 (CC49) revealed high expression throughout the entire tumor volume. This supported the observation of the high tumor fluorescence seen *in vivo* with the AlexaFluor647^{TM}+CC49 conjugate. Some positive staining of TAG72 antigen was also observed in endothelial cell-lined microvessels [Fig. 7(e)]. Staining for M195 was negative in all tumors (and other organs examined), confirming the irrelevant nature of M195 as a control MAb in these experiments. This was in agreement with the lack of appreciable tumor fluorescence *in vivo* with the AlexaFluor647^{TM}+M195 conjugate.

4. Discussion

Early endoscopic detection of small and subtle premalignant and early-staged primary gastrointestinal tumors is essential for successful cure, and increases survival rates. Conventional white-light endoscopy fails to provide sufficient image contrast for sensitive and accurate identification of early dysplastic lesions. Consequently, significant interest has evolved over the past decade in fluorescence-based and other optical imaging technologies (e.g., chromoendoscopy, narrow-band imaging, confocal microendoscopy).[3] However, to date, fluorescence endoscopy and chromoendoscopy have relied upon

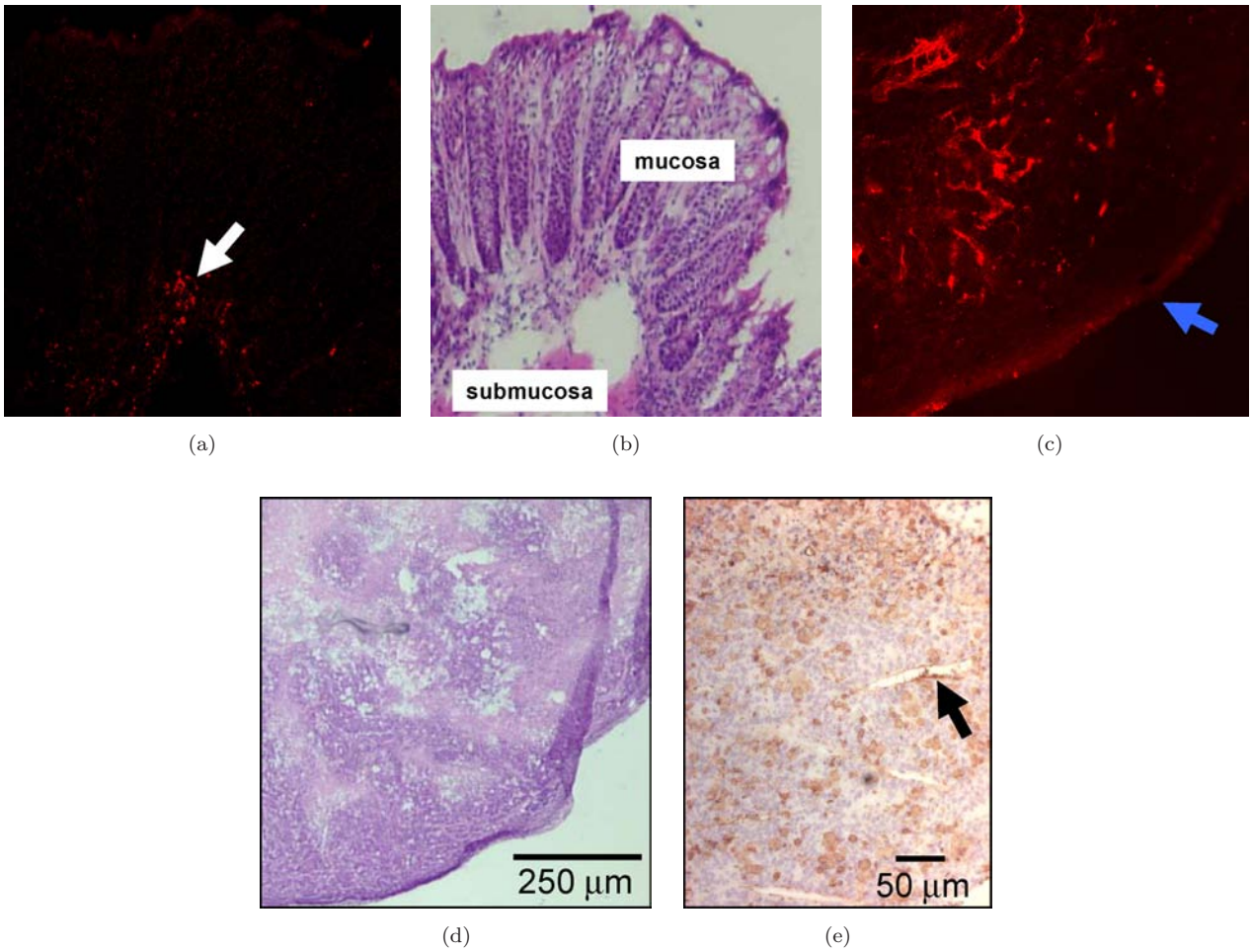

(a) (b) (c)

(d) (e)

Fig. 7. (a) and (c): Confocal fluorescence micrographs (635 nm excitation, 668 ± 15 nm emission) of *ex vivo* tissues showing the microdistribution of conjugated CC49. (a) Normal mouse colon and (b) corresponding H&E section showing very weak autofluorescence of the normal colonic epithelia and the slightly brighter autofluorescence from endogenous endocrine cells at the base of the normal colonic crypts (white arrow). (c) LS174T tumor (blue arrow marks tumor edge), (d) corresponding H&E section, and (e) tumor section immunostained with anti-TAG72 MAb (brown) and counterstained with hematoxylin (blue) showing strong positive TAG72 expression. Some endothelial cell-lined blood vessels show weak TAG72 antigen expression (black arrow).

endogenous tissue fluorophores (autofluorescence), tumor-localizing prodrugs (such as aminolevulinic acid that generates the fluorophore protoporphyrin IX) and non-specific binding of exogenous chromogenic dyes. These have certainly increased the detection sensitivity or small lesions but there is still room for further improvement. By combining near-infrared fluorescence with the antigen-binding specificity of a monoclonal antibody, in this case CC49 with a high affinity for a tumor-associated glycoprotein (TAG72) over-expressed in colon adenocarcinoma, we have shown here that it is possible to significantly improve tumor-to-normal fluorescence contrast *in vivo*. Previous targeting studies using fluorophore-antibody probes have been reported in various animal tumor models,[37,38] including for gastrointestinal cancers.[39,40] Thus, Bando *et al.* (2002) first investigated the use of a anti-MUC1 conjugate to image mucin expression in human gastrointestinal tumor tissues but this was limited to *ex vivo* tissue analysis onl.[41]

In this study, using a commercially-available conjugation kit, we have demonstrated that conjugation of a NIR fluorescent dye to the monoclonal antibody CC49 did not alter the optical properties of the dye nor the antibody specificity or antigen-binding affinity. *In vitro* imaging in LS174T cells that over-express TAG72 antigen showed bright and specific cell surface membrane labeling with as little as ∼20 ng/uL of conjugate. This was the case also in *ex vivo* LS174T tumor sections, and immunohistological staining with anti-TAG72

MAb also showed similar positive TAG72 heterogeneous expression. However, a small subpopulation of LS174T tumor cells did not express the TAG72 antigen: heterogeneity of expression may be an inherent characteristic of these cells,[42] while heterogeneous microdistribution of the fluorescent-CC49 in the LS174T tumor tissue may be due to intrinsic cell variability or differences in antigen density and/or penetration of the fluorescent probe. Nevertheless, although homogeneous antigen expression is desirable for antibody targeting, it is not critical for fluorescence-based diagnosis, since even partial expression of an antigen in a tumor will still result in successful targeted detection.[42,43]

The 2D imaging done here permitted only semi-quantitative fluorescence intensity measurements. Future studies may employ tomographic techniques for more quantitative results.[44] However, for fluorescence endoscopy the limited light penetration in tissue (even with NIR excitation) is well suited for detection of small superficial epithelial lesions (e.g., flat adenomas and dysplastic polyps in the colon), for which there are various quantification algorithms that can be applied.[45] Also, in this study the contrast agents were delivered systemically but it would be possible to apply them topically as with chromogenic dyes,[46] although it might then be necessary to employ also a mucolytic or penetration-enhancing agent.[47,48] More interestingly, novel strategies such as the use of pathogen-based delivery may be considered.[49] In either case, further research is required to evaluate the *in vivo* utility of topical application of targeted fluorescence contrast agents, and advances in confocal fluorescence microendoscopy may be an enabling technology for these studies.[50]

The use of NIR fluorescence dyes and appropriate optical filters reduces the confounding tissue autofluorescence compared with the use of visible fluorophores. However, here the use of 635-nm excitation light produced bright red fluorescence from endogenous bacterial porphyrins in the gut. This could be avoided by selecting a fluorescent dye with a somewhat longer excitation.

Since the TAG72 antigen is highly expressed in colonic dysplasia[51] and adenocarcinoma compared with normal tissue and benign hyperplastic lesions, the fluorescent CC49 probe could be useful clinically. The tendency for TAG72 expression to increase with more severe degrees of dysplasia[52] suggests that the expression of this gene product correlates with the dysplasia-to-carcinoma sequence, thus implying that TAG72 would be an ideal fluorescence contrast agent for detecting early pre-malignant lesions as well as late staged cancers. The frequent expression of TAG72 in actively inflamed colonic mucosa (ulcerative colitis and other colitides) may limit the clinical utility of this antigen for detecting colon cancer in ulcerative colitis patients by *in vivo* fluorescence localization techniques.[52] It should be noted that although the CC49 used in this study was a murine antibody, the recent construction and clinical evaluation of a humanized version of CC49 (e.g., HuCC49DeltaCH2) is promising for future clinical use.[53–55]

Distinct tumor fluorescence contrast was observed in the LS174T tumors as early as three hours post administration of the conjugate, suggesting the possibility of a "same-day" diagnostic procedure. Such fluorescence contrast agents may also be useful for guiding the endoscopic mucosal resection,[56,57] since any residual tumor at the margins could potentially be visualized. This has already been demonstrated intraoperatively using radiolabeled antibody to the TAG72 antigen (CC49) to assess the extent of colorectal carcinoma in patients.[55,58]

The metastatic behavior of LS174T cells has been well documented.[59,60] Our fluorescent-CC49 probe detected a 1-mm diameter microscopic satellite LS174T lesion, suggesting that it may also be potentially useful for detecting very small lesions as well as metastases from primary colorectal cancers, although further studies are required to confirm this. Furthermore, the CC49 antibody has been used both intraoperatively with radioimmunoguided surgery[58] and immunohistochemically[61] for detection of occult colon cancer micrometastases. Additionally, the TAG72 antigen is also highly expressed in ovarian and breast cancers, suggesting further potential applications.[62]

To the best of our knowledge, this is the first study to report non-invasive fluorescence imaging of relative TAG72-expression in human colon cancer *in vivo*. Compared with using a radiolabeled form of CC49 with a gamma detecting probe (i.e., radioimmunoguided surgery), our fluorescence-based approach is especially compatible with clinical endoscopic diagnostic imaging. Despite the fact that radioimmunoguided imaging may permit detection of deeper tumors, fluorescence endoscopic imaging offers the advantage of higher spatial resolution and is especially useful for

detecting fluorescence from the superficial mucosal layer where most early intra-epithelial lesions arise.[63] Another advantage is that using fluorescent CC49 would avoid the inherent safety concerns and complications associated with radioactive probes. In addition, whereas the use of radiolabeled CC49 would require invasive exploratory surgery which is incompatible with large-scale colon cancer screening, a fluorescent form of CC49 combined with fluorescence endoscopy potentially offers a minimally invasive imaging approach compatible with population screening protocols.

There are several other planned improvements in the work to date. First, the single intravenous dose of fluorescence-conjugated CC9 used was based on previous studies using radiolabeled CC49 (private communication, Dr. R. Reilly, Toronto). Unlike previous reports involving fluorescent antibody conjugates in which substantial quantities of protein were injected (typically $\sim 100\,\mu$g per mouse),[37,38] we used only $\sim 30\,\mu$g of dye-labeled antibody per animal — it may be useful to determine the dose-dependence of the tumor-to-normal fluorescence contrast *in vivo*. Second, the use of whole monoclonal antibodies has been associated with sub-optimal tumor penetrance,[64,65] so that future investigations should also consider the use of CC49 antibody fragments[66,67] or peptide ligands for tumor-associated TAG72 antigen[68] that should have better penetrance as well as faster tumor uptake and clearance.[69,70] Third, further optimization of the fluorophore-to-antibody binding ratios may also improve accumulation of the contrast probe in the tumors by reducing the overall size of the probe for the best possible tumor penetration.[71] Additionally, cytokine-based tumor antigen augmentation is one approach to improve the effectiveness of MAb-directed diagnosis[72]: for example, interferon-γ has been used to enhance tumor-associated glycoprotein-72 expression, thereby augmenting the antitumor effects of radioimmunoconjugate.[72,73] Also, "multimodal" contrast agents may also be designed, by coupling a fluorescent dye with magnetic iron-oxide nanoparticles for magnetic resonance imaging.[74] Such nanoprobes could potentially be used to image endoscopic surgical resections of GI tumors in real time and to correlate pre-operative MR images with intraoperative pathology at cellular-level resolution. Also, the possibility of simultaneous imaging of multiple tumor biomarkers using a cocktail of spectrally-distinct fluorescent dyes, each conjugated to different antibodies, is under investigation in our laboratory.

In conclusion, this study successfully used a highly sensitive NIR fluorescent monoclonal antibody which targeted an over-expressed human colon tumor-associated mucin to demonstrate a significant enhancement in tumor-to-normal fluorescence contrast *in vivo*. The bioconjugate retained strong affinity for the TAG72 antigen, sufficiently evaded systemic biodegradation and specifically targeted the TAG72 antigen at the LS174T tumor site. This study represents a basis for future improvements for detection of early pre-malignant lesions during endoscopy, in monitoring of disease progression and metastases, and in image-based guidance of therapeutic intervention (e.g., endoscopic mucosal resection).

Acknowledgments

This work was supported by the Ontario Research and Development Challenge Fund (ORDCF). The authors wish to thank Anoja Giles, Bob Kuba, Annie Lin and Kelvin Ho for their technical assistance.

References

1. S. Bensen, L. A. Mott, B. Dain, R. Rothstein, J. Baron, "The colonoscopic miss rate and true one-year recurrence of colorectal neoplastic polyps. Polyp Prevention Study Group," *Am. J. Gastroenterol.* **94**(1), 194–199 (1999).
2. J. C. van Rijn, J. B. Reitsma, J. Stoker, P. M. Bossuyt, S. J. van Deventer, E. Dekker, "Polyp miss rate determined by tandem colonoscopy: A systematic review," *Am. J. Gastroenterol.* **101**(2), 343–350 (2006).
3. R. S. DaCosta, B. C. Wilson, N. E. Marcon, "Optical techniques for the endoscopic detection of dysplastic colonic lesions," *Curr. Opin. Gastroenterol.* **21**(1), 70–79 (2005).
4. R. S. DaCosta, B. C. Wilson, N. E. Marcon, "New optical technologies for earlier endoscopic diagnosis of premalignant gastrointestinal lesions," *J. Gastroenterol. Hepatol.* **17**, S85–104 (2002).
5. J. Haringsma, G. N. Tytgat, H. Yano, H. Iishi, M. Tatsuta, T. Ogihara, H. Watanabe, N. Sato, N. Marcon, B. C. Wilson, R. W. Cline, "Autofluorescence endoscopy: Feasibility of detection of GI neoplasms unapparent to white light endoscopy with an evolving technology," *Gastrointest. Endosc.* **53**(6), 642–650 (2001).
6. M. Kara, R. S. DaCosta, B. C. Wilson, N. E. Marcon, J. Bergman, "Autofluorescence-based detection

of early neoplasia in patients with Barrett's esophagus," *Dig. Dis.* **22**(2), 134–141 (2004).
7. S. Brand, T. D. Wang, K. T. Schomacker, J. M. Poneros, G. Y. Lauwers, C. C. Compton, M. C. Pedrosa, N. S. Nishioka, "Detection of high-grade dysplasia in Barrett's esophagus by spectroscopy measurement of 5-aminolevulinic acid-induced protoporphyrin IX fluorescence," *Gastrointest. Endosc.* **56**(4), 479–487 (2002).
8. B. Mayinger, S. Neidhardt, H. Reh, P. Martus, E. G. Hahn, "Fluorescence induced with 5-aminolevulinic acid for the endoscopic detection and follow-up of esophageal lesions," *Gastrointest. Endosc.* **54**(5), 572–578 (2001).
9. H. Messmann, "5-aminolevulinic acid-induced protoporphyrin IX for the detection of gastrointestinal dysplasia," *Gastrointest. Endosc. Clin. N. Am.* **10**(3), 497–512 (2000).
10. L. Gossner, M. Stolte, R. Sroka, K. Rick, A. May, E. G. Hahn, C. Ell, "Photodynamic ablation of high-grade dysplasia and early cancer in Barrett's esophagus by means of 5-aminolevulinic acid," *Gastroenterology* **114**(3), 448–455 (1998).
11. W. C. Tan, C. Fulljames, N. Stone, A. J. Dix, N. Shepherd, D. J. Roberts, S. B. Brown, N. Krasner, H. Barr, "Photodynamic therapy using 5-aminolaevulinic acid for oesophageal adenocarcinoma associated with Barrett's metaplasia," *J. Photochem. Photobiol. B.* **53**(1–3), 75–80 (1999).
12. R. Ackroyd, N. J. Brown, M. F. Davis, T. J. Stephenson, C. J. Stoddard, M. W. Reed, "Aminolevulinic acid-induced photodynamic therapy: Safe and effective ablation of dysplasia in Barrett's esophagus," *Dis. Esophagus.* **13**(1), 18–22 (2000).
13. H. Messmann, R. Knuchel, W. Baumler, A. Holstege, J. Scholmerich, "Endoscopic fluorescence detection of dysplasia in patients with Barrett's esophagus, ulcerative colitis, or adenomatous polyps after 5-aminolevulinic acid-induced protoporphyrin IX sensitization," *Gastrointest. Endosc.* **49**(1), 97–101 (1999).
14. S. B. Ho, Y. S. Kim, "Carbohydrate antigens on cancer-associated mucin-like molecules," *Semin. Cancer Biol.* **2**(6), 389–400 (1991).
15. Y. S. Kim, "Altered glycosylation of mucin glycoproteins in colonic neoplasia," *J. Cell. Biochem.* **16**, 91–96 (1992).
16. N. Aksoy, O. F. Akinci, "Mucin macromolecules in normal, adenomatous, and carcinomatous colon: Evidence for the neotransformation," *Macromol. Biosci.* **4**(5), 483–496 (2004).
17. S. E. Baldus, F. G. Hanisch, "Biochemistry and pathological importance of mucin-associated antigens in gastrointestinal neoplasia," *Adv. Cancer Res.* **79**, 201–248 (2000).
18. C. R. Boland, C. K. Montgomery, Y. S. Kim, "Alterations in human colonic mucin occurring with cellular differentiation and malignant transformation," *Proc. Natl. Acad. Sci. U.S.A.* **79**(6), 2051–2055 (1982).
19. J. C. Byrd, R. S. Bresalier, "Mucins and mucin binding proteins in colorectal cancer," *Cancer Metastasis Rev.* **23**(1–2), 77–99 (2004).
20. S. B. Ho, S. L. Ewing, C. K. Montgomery, Y. S. Kim, "Altered mucin core peptide immunoreactivity in the colon polyp-carcinoma sequence," *Oncol. Res.* **8**(2), 53–61 (1996).
21. D. J. Buchsbaum, M. B. Khazaeli, M. S. Mayo, P. L. Roberson, "Comparison of multiple bolus and continuous injections of 131I-labeled CC49 for therapy in a colon cancer xenograft model," *Clin. Cancer Res.* **5**(10 Suppl), 3153s–3159s (1999).
22. F. Guadagni, M. Roselli, M. Cosimelli, P. Ferroni, A. Spila, F. Cavaliere, R. Arcuri, S. Carlini, S. Mariotti, G. M. Gandolfo, C. U. Casciani, J. W. Greiner, J. Schlom, "TAG72 expression and its role in the biological evaluation of human colorectal cancer," *Anticancer Res.* **16**(4B), 2141–2148 (1996).
23. M. Roselli, F. Guadagni, O. Buonomo, A. Belardi, P. Ferroni, A. Diodati, D. Anselmi, C. Cipriani, C. U. Casciani, J. Greiner, J. Schlom, "Tumor markers as targets for selective diagnostic and therapeutic procedures," *Anticancer Res.* **16**(4B), 2187–2192 (1996).
24. D. J. Yang, E. E. Kim, T. Inoue, "Targeted molecular imaging in oncology," *Ann. Nucl. Med.* **20**(1), 1–11 (2006).
25. S. H. Britz-Cunningham, S. J. Adelstein, "Molecular targeting with radionuclides: State of the science," *J. Nucl. Med.* **44**(12), 1945–1961 (2003).
26. R. F. Meredith, A. J. Bueschen, M. B. Khazaeli, W. E. Plott, W. E. Grizzle, R. H. Wheeler, J. Schlom, C. D. Russell, T. Liu, A. F. LoBuglio, "Treatment of metastatic prostate carcinoma with radiolabeled antibody CC49," *J. Nucl. Med.* **35**(6), 1017–1022 (1994).
27. C. R. Divgi, A. M. Scott, L. Dantis, P. Capitelli, K. Siler, S. Hilton, R. D. Finn, N. Kemeny, D. Kelsen, L. Kostakoglu *et al.*, "Phase I radioimmunotherapy trial with iodine-131-CC49 in metastatic colon carcinoma," *J. Nucl. Med.* **36**(4), 586–592 (1995).
28. R. J. Domingo, R. M. Reilly, "Pre-targeted radioimmunotherapy of human colon cancer xenografts in athymic mice using streptavidin-CC49 monoclonal antibody and 90Y-DOTA-biotin," *Nucl. Med. Commun.* **21**(1), 89–96 (2000).
29. D. J. Buchsbaum, B. E. Rogers, M. B. Khazaeli, M. S. Mayo, D. E. Milenic, S. V. Kashmiri, C. J. Anderson, L. L. Chappell, M. W. Brechbiel, D. T. Curiel, "Targeting strategies for cancer radiotherapy," *Clin. Cancer Res.* **5**(10 Suppl), 3048s–3055s (1999).

30. D. Buchsbaum, M. B. Khazaeli, T. Liu, S. Bright, K. Richardson, M. Jones, R. Meredith, "Fractionated radioimmunotherapy of human colon carcinoma xenografts with 131I-labeled monoclonal antibody CC49," *Cancer Res.* **55**(23 Suppl), 5881s–5887s (1995).
31. B. Ballou, G. W. Fisher, T. R. Hakala, D. L. Farkas, "Tumor detection and visualization using cyanine fluorochrome-labeled antibodies," *Biotechnol. Prog.* **13**(5), 649–658 (1997).
32. V. Ntziachristos, "Fluorescence molecular imaging," *Annu. Rev. Biomed. Eng.* **8**, 1–33 (2006).
33. D. C. Andersen, D. E. Reilly, "Production technologies for monoclonal antibodies and their fragments," *Curr. Opin. Biotechnol.* **15**(5), 456–462 (2004).
34. A. Thor, N. Ohuchi, C. A. Szpak, W. W. Johnston, J. Schlom, "Distribution of oncofetal antigen tumor-associated glycoprotein-72 defined by monoclonal antibody B72.3," *Cancer Res.* **46**(6), 3118–3124 (1986).
35. H. Andersson, T. Baechi, M. Hoechl, C. Richter, "Autofluorescence of living cells," *J. Microsc.* **191**(Pt 1), 1–7 (1998).
36. R. DaCosta, "Mechanisms of fluorescence endoscopy of the human colon," in Department of Medical Biophysics, University of Toronto, Toronto, Ontario, Canada (1999).
37. B. Ballou, G. W. Fisher, A. S. Waggoner, D. L. Farkas, J. M. Reiland, R. Jaffe, R. B. Mujumdar, S. R. Mujumdar, T. R. Hakala, "Tumor labeling *in vivo* using cyanine-conjugated monoclonal antibodies," *Cancer Immunol. Immunother.* **41**(4), 257–263 (1995).
38. S. Folli, P. Westermann, D. Braichotte, A. Pelegrin, G. Wagnieres, H. van den Bergh, J. P. Mach, "Antibody-indocyanin conjugates for immunophotodetection of human squamous cell carcinoma in nude mice," *Cancer Res.* **54**(10), 2643–2649 (1994).
39. S. Ito, N. Muguruma, Y. Kusaka, M. Tadatsu, K. Inayama, Y. Musashi, M. Yano, T. Bando, H. Honda, I. Shimizu, K. Ii, K. Takesako, H. Takeuchi, S. Shibamura, "Detection of human gastric cancer in resected specimens using a novel infrared fluorescent anti-human carcinoembryonic antigen antibody with an infrared fluorescence endoscope *in vitro*," *Endoscopy* **33**(10), 849–853 (2001).
40. N. Muguruma, S. Ito, T. Bando, S. Taoka, Y. Kusaka, S. Hayashi, S. Ichikawa, Y. Matsunaga, Y. Tada, S. Okamura, K. Ii, K. Imaizumi, K. Nakamura, K. Takesako, S. Shibamura, "Labeled carcinoembryonic antigen antibodies excitable by infrared rays: A novel diagnostic method for microcancers in the digestive tract," *Intern. Med.* **38**(7), 537–542 (1999).
41. T. Bando, N. Muguruma, S. Ito, Y. Musashi, K. Inayama, Y. Kusaka, M. Tadatsu, I. Kunio, T. Irimura, S. Shibamura, K. Takesako, "Basic studies on a labeled anti-mucin antibody detectable by infrared-fluorescence endoscopy," *J. Gastroenterol.* **37**(4), 260–269 (2002).
42. P. Carter, L. Smith, M. Ryan, "Identification and validation of cell surface antigens for antibody targeting in oncology," *Endocr. Relat. Cancer* **11**(4), 659–687 (2004).
43. P. A. Edwards, "Heterogeneous expression of cell-surface antigens in normal epithelia and their tumours, revealed by monoclonal antibodies," *Br. J. Cancer* **51**(2), 149–160 (1985).
44. X. Montet, V. Ntziachristos, J. Grimm, R. Weissleder, "Tomographic fluorescence mapping of tumor targets," *Cancer Res.* **65**(14), 6330–6336 (2005).
45. A. Bogaards, "*In vivo* fluorescence imaging of markers for detection and guided resection of cancer," Erasmus University, Rotterdam, The Netherlands (2006).
46. J. H. Lee, J. W. Kim, Y. K. Cho, C. I. Sohn, W. K. Jeon, B. I. Kim, E. Y. Cho, "Detection of colorectal adenomas by routine chromoendoscopy with indigocarmine," *Am. J. Gastroenterol.* **98**(6), 1284–1288 (2003).
47. H. Sezaki, "Mucosal penetration enhancement," *J. Drug. Target.* **3**(3), 175–177 (1995).
48. S. Takatsuka, T. Kitazawa, T. Morita, Y. Horikiri, H. Yoshino, "Enhancement of intestinal absorption of poorly absorbed hydrophilic compounds by simultaneous use of mucolytic agent and non-ionic surfactant," *Eur. J. Pharm. Biopharm.* **62**(1), 52–58 (2006).
49. K. P. Janssen, D. Vignjevic, R. Boisgard, T. Falguieres, G. Bousquet, D. Decaudin, F. Dolle, D. Louvard, B. Tavitian, S. Robine, L. Johannes, "*In vivo* tumor targeting using a novel intestinal pathogen-based delivery approach," *Cancer Res.* **66**(14), 7230–7236 (2006).
50. R. Kiesslich, M. Goetz, M. Vieth, P. R. Galle, M. F. Neurath, "Confocal laser endomicroscopy," *Gastrointest. Endosc. Clin. N. Am.* **15**(4), 715–731 (2005).
51. B. C. Wolf, J. C. D'Emilia, R. R. Salem, D. DeCoste, H. F. Sears, L. S. Gottlieb, G. D. Steele, Jr., "Detection of the tumor-associated glycoprotein antigen (TAG72) in premalignant lesions of the colon," *J. Natl. Cancer Inst.* **81**(24), 1913–1917 (1989).
52. A. Thor, S. H. Itzkowitz, J. Schlom, Y. S. Kim, S. Hanauer, "Tumor-associated glycoprotein (TAG72) expression in ulcerative colitis," *Int. J. Cancer* **43**(5), 810–815 (1989).
53. B. E. Rogers, P. L. Roberson, S. Shen, M. B. Khazaeli, M. Carpenter, S. Yokoyama, M. W. Brechbiel, A. F. LoBuglio, D. J. Buchsbaum, "Intraperitoneal radioimmunotherapy with a humanized anti-TAG72

(CC49) antibody with a deleted CH_2 region," *Cancer Biother. Radiopharm.* **20**(5), 502–513 (2005).
54. J. Xiao, S. Horst, G. Hinkle, X. Cao, E. Kocak, J. Fang, D. Young, M. Khazaeli, D. Agnese, D. Sun, E. Martin, Jr., "Pharmacokinetics and clinical evaluation of 125I-radiolabeled humanized CC49 monoclonal antibody (HuCC49deltaC(H)2) in recurrent and metastatic colorectal cancer patients," *Cancer Biother. Radiopharm.* **20**(1), 16–26 (2005).
55. D. M. Agnese, S. F. Abdessalam, W. E. Burak, Jr., M. W. Arnold, D. Soble, G. H. Hinkle, D. Young, M. B. Khazaeli, E. W. Martin, Jr., "Pilot study using a humanized CC49 monoclonal antibody (HuCC49DeltaCH2) to localize recurrent colorectal carcinoma," *Ann. Surg. Oncol.* **11**(2), 197–202 (2004).
56. M. A. Ortner, G. Dorta, A. L. Blum, P. Michetti, "Endoscopic interventions for preneoplastic and neoplastic lesions: Mucosectomy, argon plasma coagulation, and photodynamic therapy," *Dig. Dis.* **20**(2), 167–172 (2002).
57. R. H. Hawes, "Perspectives in endoscopic mucosal resection," *Gastrointest. Endosc. Clin. N. Am.* **11**(3), 549–552 (2001).
58. R. J. Cote, D. P. Houchens, C. L. Hitchcock, A. D. Saad, R. G. Nines, J. K. Greenson, S. Schneebaum, M. W. Arnold, E. W. Martin, Jr., "Intraoperative detection of occult colon cancer micrometastases using 125I-radiolabeled monoclonal antibody CC49," *Cancer* **77**(4), 613–620 (1996).
59. K. Ikawa, Y. Terashima, K. Sasaki, S. Tashiro, "Genetic detection of liver micrometastases that are undetectable histologically," *J. Surg. Res.* **106**(1), 124–130 (2002).
60. M. J. Koppe, A. C. Soede, W. Pels, W. J. Oyen, D. M. Goldenberg, R. P. Bleichrodt, O. C. Boerman, "Experimental radioimmunotherapy of small peritoneal metastases of colorectal origin," *Int. J. Cancer* **106**(6), 965–972 (2003).
61. J. K. Greenson, C. E. Isenhart, R. Rice, C. Mojzisik, D. Houchens, E. W. Martin, Jr., "Identification of occult micrometastases in pericolic lymph nodes of Duke's B colorectal cancer patients using monoclonal antibodies against cytokeratin and CC49. Correlation with long-term survival," *Cancer* **73**(3), 563–569 (1994).
62. R. Muraro, M. Kuroki, D. Wunderlich, D. J. Poole, D. Colcher, A. Thor, J. W. Greiner, J. F. Simpson, A. Molinolo, P. Noguchi *et al.*, "Generation and characterization of B72.3 second generation monoclonal antibodies reactive with the tumor-associated glycoprotein 72 antigen," *Cancer Res.* **48**(16), 4588–4596 (1988).
63. M. Guindi, R. H. Riddell, "The pathology of epithelial pre-malignancy of the gastrointestinal tract," *Best Pract. Res. Clin. Gastroenterol.* **15**(2), 191–210 (2001).
64. F. Yuan, M. Leunig, D. A. Berk, R. K. Jain, "Microvascular permeability of albumin, vascular surface area, and vascular volume measured in human adenocarcinoma LS174T using dorsal chamber in SCID mice," *Microvasc. Res.* **45**(3), 269–289 (1993).
65. F. Yuan, M. Dellian, D. Fukumura, M. Leunig, D. A. Berk, V. P. Torchilin, R. K. Jain, "Vascular permeability in a human tumor xenograft: Molecular size dependence and cutoff size," *Cancer Res.* **55**(17), 3752–3756 (1995).
66. S. M. Larson, A. M. El-Shirbiny, C. R. Divgi, G. Sgouros, R. D. Finn, J. Tschmelitsch, A. Picon, M. Whitlow, J. Schlom, J. Zhang, A. M. Cohen, "Single chain antigen binding protein (sFv CC49): First human studies in colorectal carcinoma metastatic to liver," *Cancer* **80**(12 Suppl), 2458–2468 (1997).
67. Y. Tang, S. Yang, J. Gariépy, D. Scollard, R. Reilly, "Construction and evaluation of the tumor imaging properties of 123I-labeled recombinant and enzymatically-generated Fab fragments of the TAG72 monoclonal antibody CC49," *Bioconjug. Chem.* **18**(3), 677–684 (2007).
68. J. Gui, T. Moyana, B. Malcolm, J. Xiang, "Identification of a decapeptide with the binding reactivity for tumor-associated TAG72 antigen from a phage displayed library," *Proteins* **24**(3), 352–358 (1996).
69. A. Becker, C. Hessenius, K. Licha, B. Ebert, U. Sukowski, W. Semmler, B. Wiedenmann, C. Grotzinger, "Receptor-targeted optical imaging of tumors with near-infrared fluorescent ligands," *Nat. Biotechnol.* **19**(4), 327–331 (2001).
70. K. Kelly, H. Alencar, M. Funovics, U. Mahmood, R. Weissleder, "Detection of invasive colon cancer using a novel, targeted, library-derived fluorescent peptide," *Cancer Res.* **64**(17), 6247–6251 (2004).
71. R. K. Jain, "Transport of molecules, particles, and cells in solid tumors," *Annu. Rev. Biomed. Eng.* **1**, 241–263 (1999).
72. J. W. Greiner, F. Guadagni, M. Roselli, C. A. Nieroda, "Novel approaches to tumor detection and therapy using a combination of monoclonal antibody and cytokine," *Anticancer Res.* **16**(4B), 2129–2133 (1996).
73. M. Roselli, F. Guadagni, O. Buonomo, A. Belardi, V. Vittorini, R. Mariani-Costantini, J. W. Greiner, C. U. Casciani, J. Schlom, "Systemic administration of recombinant interferon alfa in carcinoma patients upregulates the expression of the carcinoma-associated antigens tumor-associated glycoprotein-72 and carcinoembryonic antigen," *J. Clin. Oncol.* **14**(7), 2031–2042 (1996).
74. O. Veiseh, C. Sun, J. Gunn, N. Kohler, P. Gabikian, D. Lee, N. Bhattarai, R. Ellenbogen, R. Sze, A. Hallahan, J. Olson, M. Zhang, "Optical and MRI multifunctional nanoprobe for targeting gliomas," *Nano Lett.* **5**(6), 1003–1008 (2005).